

# CONSTRAINTS ON THE DELAYED TRANSITION TO DETONATION IN TYPE Ia SUPERNOVAE

A. M. LISEWSKI AND W. HILLEBRANDT

Max-Planck-Institut für Astrophysik, Karl-Schwarzschild-Straße 1, 85740 Garching, Germany

AND

S. E. WOOSLEY

UCO/Lick Observatory, University of California Santa Cruz, Santa Cruz, CA 95064

Received 1999 October 11; accepted 2000 January 12

## ABSTRACT

We investigate the possibility of a delayed detonation in a Type Ia supernova under the assumption that the transition to detonation is triggered by turbulence only. Our discussion is based on the Zeldovich mechanism and suggests that typical turbulent velocities present during the explosion are not strong enough to allow this transition to occur. Although we are able to show that in carbon-rich matter (e.g.,  $X(^{12}\text{C}) = 0.75$ ) the possibility of a deflagration to detonation transition (DDT) is enhanced, even in this case, the turbulent velocities needed are larger than the expected value of  $u'(L) \approx 10^7 \text{ cm s}^{-1}$  on a length-scale of  $L \approx 10^6 \text{ cm}$ . Thus we conclude that a DDT may not be a common event during a thermonuclear explosion of a Chandrasekhar-mass white dwarf.

*Subject headings:* shock waves — supernovae: general — turbulence

## 1. INTRODUCTION

The question whether a detonation occurs during the thermonuclear explosion of a white dwarf of Chandrasekhar mass has already been discussed extensively. Many existing models assume that such a transition does occur in certain situations during the explosion. Some of these models, the so-called delayed-detonation models, assume that at a critical value of a model parameter (usually the density) a previously subsonic burning front turns into a detonation. In comparison with observables, like light-curve shape, peak brightness, or element abundances, the delayed-detonation scenario seemed to comply well (e.g., Höflich et al. 1996). However, a conclusive answer to whether this transition is physically possible has not been given yet.

In a thermonuclear supernova, the explosion energy is produced by a moving thermonuclear flame that burns carbon and oxygen into higher mass elements. According to our present understanding, at least at high densities, i.e., in the inner core ( $\rho > 10^8 \text{ g cm}^{-3}$ ) of the white dwarf, the burning mode of this flame is a deflagration, where the burning front can locally be described as a laminar flame. The properties of laminar flames in white dwarf matter are well known (Timmes & Woosley 1992). One general feature is that with lower density the speed of a laminar flame decreases rapidly while at the same time its thickness increases. On the other hand, numerical models of Type Ia supernovae tailored to reproduce light curves and spectra require a flame velocity that is nearly independent of the density in the unburned material. Thus there must be a mechanism that leads to an effective flame velocity being independent of its laminar properties. It is commonly believed that turbulence provides this mechanism. However, quantitative predictions of the turbulent flame velocity are not easy to obtain because they depend on many (often very uncertain) parameters such as density, nuclear compositions, turbulent properties, etc. It is not even clear if the flame speed remains always subsonic or if it might turn into a detonation. Leaving out scenarios like the prompt initial detonation (see, e.g., Imshennik et al. 1999, and references therein) and the pulsating delayed detona-

tion (e.g., Khokhlov et al. 1997), we focus on the problem of whether turbulence alone is able to trigger a supersonic burning wave accompanied by a hydrodynamic shock.

In order to achieve this goal, we introduce a method to represent the structure of a flame moving through a turbulent medium. For a given physical state of the unburned matter, and for a specified turbulent energy, the model adopts the most optimistic assumptions for the transition from a deflagration to a detonation. We then investigate if such a transition happens under these special prerequisites. Cases in which no transition is observed therefore provide quantitative limits on some relevant physical parameters, such as nuclear composition or turbulence intensity. These limits constrain the regime where a detonation triggered by turbulence might occur.

This paper is structured as follows. First, we briefly recall some properties of carbon flames at densities around  $10^7 \text{ g cm}^{-3}$  where, according to our present understanding (see, e.g. Khokhlov et al. 1997 and Niemeyer & Woosley 1997), the chances of a DDT are the highest. Then we introduce our method to represent turbulence effects on subsonic flames. In this way we obtain some turbulent flame profiles which we eventually implement as initial conditions in a gasdynamic system to study their temporal evolution. Finally, we discuss some implications of our results.

## 2. THE MODEL

The structure of a flame moving through a turbulent medium crucially depends on the characteristic turbulent length scales, such as the scale where the biggest turbulent motions are produced and the dissipation scale where turbulent motion is smeared out by microscopic diffusion, as well as on the amount of turbulent kinetic energy that drives the turbulent motion. Of course, in case of turbulence driven by inertia these scales become the inertial scale  $L$  and the Kolmogorov scale  $l_k$ . On the other hand, it is important to know how these typical turbulent entities relate to the given chemical and thermodynamical properties that are responsible for the burning process itself.

Here we set up a model that represents this relation in a certain way. Consider a flame—laminar or turbulent—in the incompressible case, that is, a flame with no pressure jump across it. Then the burned and unburned states of matter are given by the density, temperature, and nuclear composition of the unburned state and by the available amount of energy released by nuclear reactions under these conditions. The only difference between a turbulent and a laminar flame is the spatial and temporal distribution of density, temperature, and nuclear abundances within the interface between fuel and ashes, i.e., the flame profile. For instance, in a laminar flame temperature is a monotonically decreasing function in the direction of the unburned material, whereas in the turbulent case fluctuations can cause this function to have sharp spikes and dips.

Turbulence has two main impacts on the burning process. First, there is an enlargement of the flame surface caused by turbulent stretching and wrinkling, leading to a higher effective flame speed. Second, in cases of higher turbulence intensity, vortices can even mix burned or burning material with unburned matter. This happens when they are fast enough to carry reactive material away from the flame before this material is burned completely. As a direct consequence one observes a broadening of the flame profile. Now the flame structure is superposed by fluctuations coming from turbulent motion. However, in this work we neglect a direct representation of fluctuations and instead concentrate on one net effect of the latter, namely, the enhanced heat and mass transport that actually causes the broadening of the flame. The resulting spatial structure of the flame and in particular its size play a crucial role in the DDT problem.

The profile of an incompressible laminar flame is described by the set of functions  $T_i(x, t)$ ,  $\rho_i(x, t)$ ,  $Y_{i,l}(x, t)$ , which give the spatiotemporal distributions of temperature, density, and nuclear number density of the  $i$ th species at a constant pressure  $P$ . These functions are solutions of the following system of equations:

$$\frac{\partial Y_{i,l}}{\partial t} = \sum_{j,k} -Y_{i,l} Y_{k,l} \lambda_{jk}(i) + Y_{i,l} Y_{k,l} \lambda_{kj}(i), \quad (1)$$

$$\frac{\partial T_l}{\partial t} = \frac{1}{\rho c_p} \frac{\partial}{\partial x} \left( \sigma \frac{\partial T_l}{\partial x} \right) - P \frac{\partial}{\partial t} \frac{1}{\rho} + \frac{1}{c_p} \dot{S}, \quad (2)$$

$$\dot{S} = N_A \sum_i \frac{dY_{i,l}}{dt} B_i. \quad (3)$$

Herein  $c_p = c_p(T_l, \rho_l, Y_{i,l})$  is the heat capacity,  $\sigma = \sigma(T_l, \rho_l, Y_{i,l})$  is the thermal conductivity,  $B_i$  is the binding energy, and  $Y_{i,l}$  is the number density of the  $i$ th nucleus, while  $\lambda_{ij}$  denotes the reaction rate of nuclei  $i$  and  $j$ . Our reaction network consists of seven species, viz.,  $^4\text{He}$ ,  $^{12}\text{C}$ ,  $^{16}\text{O}$ ,  $^{20}\text{Ne}$ ,  $^{24}\text{Mg}$ ,  $^{28}\text{Si}$ , and  $^{56}\text{Ni}$ .

The direction of the flame is chosen to be such that the completely burned state is at  $x = -\infty$ . In a steady state the flame represented by these equations propagates with a constant velocity  $s_l$ . Thus in a comoving frame the functions  $T_l$ ,  $\rho_l$ , and  $X_{i,l}$  are constant in time, and it is convenient to place the origin of the comoving coordinate system at the point of maximum energy generation.

The flame profile defines also a spatial distribution of the nuclear reaction timescale of the  $i$ th element,  $\tau_m(i)$ , by

$$\tau_m(i) = \left( \frac{Y_i}{\dot{Y}_i} \right)_{T,\rho}, \quad (4)$$

where the time derivative is taken at constant temperature and density. In this work we are particularly interested in C + O matter at densities around  $10^7 \text{ g cm}^{-3}$ , where by far the most relevant nuclear reaction is  $^{12}\text{C} + ^{12}\text{C}$ . Burning of heavier elements takes place on timescales much longer than  $\tau_m(^{12}\text{C})$  and releases much less energy. We will therefore always refer to carbon burning in the following.

Note that the equation (4) overestimates the nuclear burning time because burning a small fraction of the given carbon already significantly raises the temperature, which in turn increases the reaction rate. Equation (4) assumes that temperature remains constant during the reaction, neglecting any self-accelerating effects of nuclear burning. Thus to obtain a more realistic estimate on the nuclear burning time we will refer to the so-called induction time of nuclear burning. It is known (e.g., Khokhlov 1991) that the process of explosive nuclear burning can be subdivided into two temporal stages. During the first phase after ignition, at times shorter than the induction time  $\tau_i$ , the temperature increases slowly (linearly) in time, and the corresponding energy production is relatively small.

After this, during the explosive phase, energy production evolves quasi-exponentially in time. Thus only the induction time is actually needed to burn a fluid element completely because  $\tau_i$  is nearly equal to the time it takes to burn most of the fuel. Self-acceleration of nuclear burning leads to the relation  $\tau_i \ll \tau_m$ . The ratio of the induction and the constant temperature timescale can approximately be given by an analytic expression known as the Frank-Kamenetskii factor. However, for our purposes we calculate  $\tau_i$  numerically using the equation

$$\int_0^{\tau_i} \dot{Y}_{^{12}\text{C}} dt = \gamma Y_{^{12}\text{C}}(t=0), \quad (5)$$

where  $\gamma$  denotes the total fraction of burned material. Based on equation (5), Figure 1 represents the time required to burn a fraction  $(1 - \gamma)$  of the initial fuel amount, and it clearly shows that for any value  $\gamma \in [0.2, 0.9]$  this time

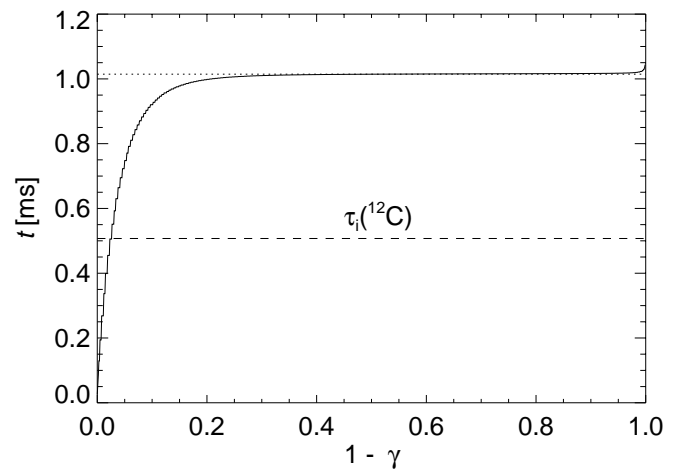


FIG. 1.—The estimated time for burning a fraction  $1 - \gamma$  of an initial carbon abundance  $X(^{12}\text{C}) = \frac{1}{2}$  at an initial temperature of  $1.7 \times 10^9 \text{ K}$  and a density of  $2.3 \times 10^7 \text{ g cm}^{-3}$ . The resulting value of the induction time,  $\tau_i$ , is shown by the dashed line.

turns out to be almost the same. We therefore use equation (5)—with an arbitrary choice of  $\gamma \in [0.2, 0.9]$ —to define the induction time  $\tau_{i,12C}$  as *half* of the time it takes to burn most of the fuel. This definition ensures that for times smaller than  $\tau_i$  the burning process evolves almost linearly.

For a phenomenological description of turbulence we assume that the turbulent velocities obey Kolmogorov's scaling law. In particular, this implies the following scaling of the rms turbulent velocity fluctuations  $u'(l)$ :

$$u'(l) = u'(L) \left( \frac{l}{L} \right)^{1/3}, \quad (6)$$

with  $l_K = L \text{Re}^{-3/4} < l < L$ , where  $L$  is the integral length scale and  $\text{Re}$  is the turbulent Reynolds number. In order to model the effect of turbulent motions on a flame front we make two additional assumptions:

1. Turbulent vortices are viewed as a transport mechanism of heat and mass. Thus a fluid element can be carried by a vortex over a distance  $l$  after a time  $\tau_l = (\frac{1}{2})[l/u'(l)]$ , which is half of the eddy's turnover time. In case of a one-dimensional and comoving representation of a flame, this mechanism transports heat and nuclear species located at  $x > 0$  in the positive direction, while fluid elements placed at  $x < 0$  are transported in the negative one.

2. Since the spatial distribution of the induction time  $\tau_i(x)$  is a single-valued function in the regions  $x > 0$  and  $x < 0$ , every fluid element has its unique value of  $\tau_i(x)$ . Then the distance  $l'_\tau$  over which a fluid element located at  $x$  can be moved is determined by the equation  $\tau_l = \tau_i$  leading to

$$l'_\tau(x) = \frac{[2u'(L)\tau_i]^{3/2}}{L^{1/2}}. \quad (7)$$

In this approach  $l'_\tau(x)$  is not allowed to exceed the integral length,  $L$ , neither should it get smaller than the Kolmogorov length,  $l_K$ <sup>1</sup>. Furthermore, because the flame itself moves on during the time  $\tau_i$  (at least with its laminar velocity  $s_l$ ), we have to subtract the distance  $s_l \tau_i$  from the original value of  $l'_\tau(x)$ . This results in the expression

$$l_\tau(x) = H[\chi_{[l_K, L]}(l'_\tau)l'_\tau - s_l \tau_i][\chi_{[l_K, L]}(l'_\tau)l'_\tau - s_l \tau_i], \quad (8)$$

where  $\chi_{[l_K, L]}$  is the characteristic function of the interval  $[l_K, L]$  (this is,  $\chi_{[l_K, L]}(x) = 1$  for  $x \in [l_K, L]$ , and 0 otherwise.) for giving a cutoff for scales smaller than  $l_K$  and larger than  $L$ .  $H$  is Heaviside's function representing the obvious fact that negative values of  $l_\tau(x)$  are not admissible.

Using equation (8), the turbulent flame profile is given by

$$\left\{ \begin{array}{ll} \{\rho_\tau, T_\tau, Y_\tau\}[x + l_\tau(x)] & x > 0 \\ \{\rho_\tau, T_\tau, Y_\tau\}[x - l_\tau(x)] & x < 0 \end{array} \right\} = \{\rho_l, T_l, Y_l\}(x). \quad (9)$$

Our first assumption was that there is additional heat/mass-transport due to turbulent eddies leading to a broadening of the flame. But it ignores the fact that turbulence is actually isotropic, which means that eddies occur in any direction without a preferred one. However, as long as the flame's reaction zone is relatively well localized there will always be a flame surface defined by the points of maximum energy production. Thus there is a preferred

direction locally defined by the normal vector of the flame surface. Turbulence randomly drags and shifts this surface but in a locally comoving frame turbulent motion increases the thermal and nuclear transport in directions normal to it. Heuristically, this can be seen by introducing a local *eddy diffusivity*  $D_i(x) = u'(x)x$ , where  $x$  denotes the distance from the flame surface. Thus turbulence imposes an enhanced heat flux ahead of the flame's surface. In the reaction region the induction times are so short that turbulent mixing hardly changes its structure. Well behind the thin reaction zone almost all of the carbon is already burned. Thus turbulent motions in regions behind this zone actually stirs pure ashes. In the context of the present work it is therefore sufficient to consider effects of turbulence only for  $x > 0$ .

One may argue that in reality there is not just one flame profile along the normal direction of a flame surface, but there is a random superposition of flames, fuels, and ashes, giving rise to strong fluctuations in temperature and nuclear abundances. However, as was stated before, we do not intend to give a full description of the structure of a turbulent flame. It is our aim to model a situation which is most favorable for carbon detonation. In order to trigger a detonation based on the Zeldovich mechanism (Zeldovich et al. 1970) one needs a region of a certain critical size with a rather uniform temperature and fuel fraction. To be more specific, a nonuniform spatial region of induction times must be present such that within this region spontaneous burning reaches a critical velocity threshold. Let  $\sigma(\tau_i)$  be the resulting variance of the induction times. Then this region must be at least of size  $\sigma(\tau_i)a_s$ , where  $a_s$  is the local sound velocity (see Khokhlov 1991). In the presence of temperature and fuel fluctuations a successful formation of such a region is strongly suppressed because the rate and the amplitude of fluctuations grow with scale. Therefore one expects that such homogeneous regions are already torn apart into smaller sections before they can ever reach the critical size (Niemeyer 1999). Our model aims at describing the unlikely situation that such strong fluctuations are not present, and therefore we could find detonations which in reality would not happen. On the other hand, if certain physical conditions described by a set of parameters  $\rho, s_l, \text{Re}, L, l_K$ , etc., make a successful detonation impossible in our model, it indicates that under the same prerequisites a detonation in a real turbulent flame would not happen either.

In order to determine a relation between turbulence intensity and the resulting shape of the flame we make one more assumption. The main motivation for it is the desire to relate an undisturbed (laminar) flame profile with a time setting a maximum limit for the turbulent transport. In fact, the maximum time for which a fluid element with a significant amount of fuel can be transported by turbulent motion is  $\tau_i$ , i.e., its induction time. During this period it covers a distance  $l'_\tau$  given by the size of a certain eddy, cf. equation (7)<sup>2</sup>. Considering this for every fluid element within a laminar flame, one can derive a formula for the shape of the turbulent flame, which is exactly equation (9). This equation already involves a simplification because we use the induction time in order to estimate  $l'_\tau$ . As mentioned above, the

<sup>1</sup> The reason why we do not consider length scales larger than  $L$  is that we actually do not know how the turbulent spectrum of velocity fluctuations looks like at long wavelengths. Rayleigh-Taylor unstable structures (bubbles) in the nonlinear stage of this instability may cause additional effects on the turbulent behavior (see, e.g., Niemeyer & Woosley 1997) leading to significant deviations from isotropy and homogeneity.

<sup>2</sup> It should be remarked that  $l'_\tau$ , given by eq. (7), is the maximum distance for turbulent transport at a given  $\tau$ . That means that bigger eddies are not able to carry a fluid element further out than  $l'_\tau$ . This can be easily verified when Kolmogorov scaling is assumed.

thermodynamic state of a fluid element changes only slightly after a period of time given by  $\tau_i$ , i.e.,  $T_i(t + \tau_i) \approx T_i(t)$  and  $Y_{12C,i}(t + \tau_i) \approx Y_{12C,i}(t)$ . Thus the state of the fluid element after being transported over a distance  $l_\tau$  is nearly the same as its original state. However, taking into account significantly longer times than  $\tau_i$  would lead to strong spatial fluctuations in temperature and composition. For instance, assume that a fluid element is transported over a distance  $l_\tau$  where  $\tau \approx 2\tau_i$ . Furthermore, consider a small fluctuation in time  $\delta\tau \ll \tau$ . Then we have  $l_{\tau \pm \delta\tau} \approx l_\tau$ , but  $T(\tau \pm \delta\tau)$  might be much bigger or smaller than  $T(\tau)$  depending on the sign of the fluctuation. Of course, spatial fluctuations in carbon composition would be even stronger in amplitude. Again, based on the same arguments as given above, these fluctuations would make the formation of a detonation much more unlikely. Therefore for the purpose of this paper it is sufficient to represent the flame-turbulence interaction in the linear regime characterized by the induction time scale.

Two of the resulting turbulent profiles are shown in Figure 2. One sees that the innermost region of the flame is hardly disturbed by turbulent motions even at turbulent velocities of  $u'(L) = 10^7 \text{ cm s}^{-1}$ . In contrast, regions of slow reactions are widely extended causing a huge preheated zone ahead of the flame.

### 3. TESTING FOR DETONATIONS

In this section we use the results stated above to implement them as initial conditions for the solution of the fully compressible hydrodynamical equations. The question then is under which conditions the flame evolves into a detonation. Similar investigations have already been done (Khokhlov 1991; Niemeyer & Woosley 1997). In these studies the initial conditions were parametrized by the width of a nonuniformly burning region. It was shown that there exists—for given density and fuel composition—a minimum (critical) length scale such that nonuniform burning on scales larger than this leads to a detonation. However, in these investigations the important question of how such a region might form was not addressed. Only weak necessary conditions limiting the strength of the turbulence-flame interaction have been given. For instance, the authors demand a *breaking up* of the flame (Khokhlov et

al. 1997) or burning in the *distributed regime* (Niemeyer & Woosley 1997).

Our model establishes a direct relation between turbulence intensity and the shape of the flame profile. Using this relation we are able to give necessary conditions for a transition to detonation.

The system of conservation laws that we solve numerically is

$$\frac{\partial \rho}{\partial t} + \nabla \cdot (\rho \mathbf{U}) = 0, \quad (10)$$

$$\frac{\partial \rho U}{\partial t} + \nabla \cdot (\rho \mathbf{U}) + \nabla P = 0, \quad (11)$$

$$\frac{\partial E}{\partial t} + \nabla \cdot [(E + P)\mathbf{U}] = 0, \quad (12)$$

$$\frac{\partial Y_i}{\partial t} + (\mathbf{U} \cdot \nabla) Y_i + \sum_{j,k} Y_i Y_k \lambda_{jk}(i) - Y_i Y_k \lambda_{kj}(i) = 0, \quad (13)$$

where  $\mathbf{U}$  is the fluid velocity and  $E = \epsilon + \rho U^2/2 + \rho N_A \sum B_i Y_i$  is the total energy density defined as the sum of the internal, the kinetic, and the binding energy term. These equations are coupled to the same equation of state and nuclear reaction network as already used in the reactive diffusion equations (1) and (2). They are solved in a one-dimensional planar geometry with outflow boundary conditions as well as in spherical geometry. In the latter case we use a reflecting inner boundary and an outflow condition on the outside. As a numerical scheme we used PROMETHEUS (Fryxell et al. 1989), a second-order explicit in time solver for reactive hydrodynamics.

We consider three different densities, namely 2.3, 1.3, and  $0.8 \times 10^7 \text{ g cm}^{-3}$ , and three different compositions of the fuel:  $X(^{12}\text{C})/X(^{16}\text{O}) = 1, \frac{1}{3}, \text{ and } 3$ . The turbulent velocity fluctuations in an exploding Chandrasekhar-mass white dwarf are (see Niemeyer & Woosley 1997; Khokhlov et al. 1997) believed to be  $u'(L) \approx 10^6\text{--}10^7 \text{ cm s}^{-1}$  on an integral length scale of  $L \approx 10^6 \text{ cm}$ . In all our numerical computations we keep the integral scale fixed at this particular value, and the only turbulent variable remains the amplitude of turbulent velocity fluctuations  $u'(L)$ .

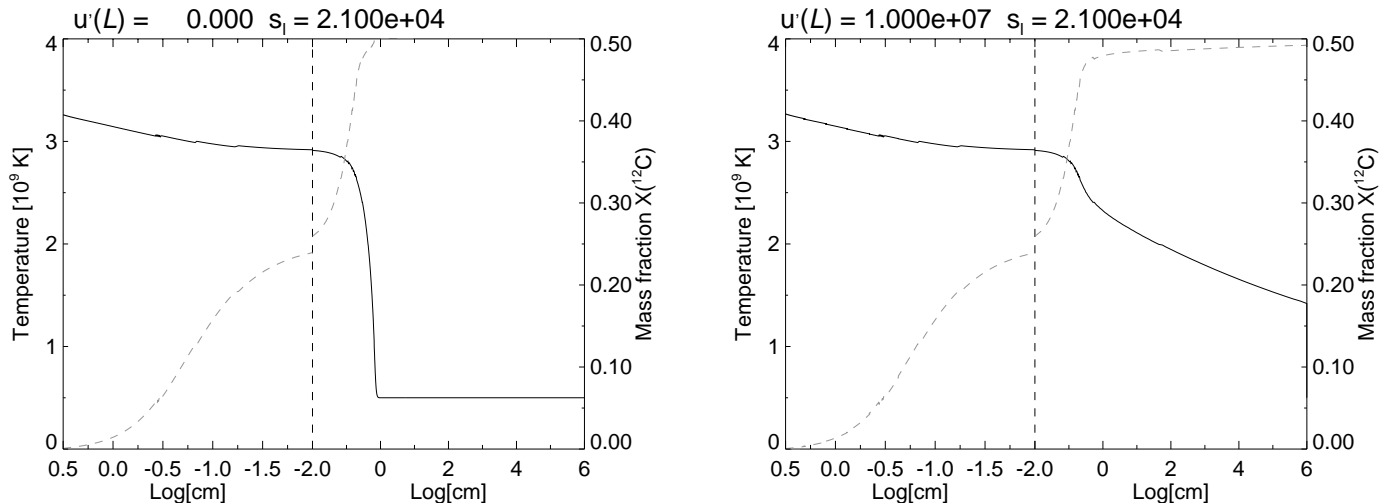


FIG. 2.—Estimated shapes of turbulent flames. A laminar flame profile (left) and a turbulent flame profile (right). Both represent a flame at a fuel density of  $2.3 \times 10^7 \text{ g cm}^{-3}$ .

Given initial conditions as described above, we need to find a natural time limit for evolving the hydrodynamics. Since the flame dynamics is embedded into the global dynamics of the star, we adopt this limit to be the hydrodynamical timescale,  $\tau_h$ , of the exploding white dwarf. After this time has elapsed, the stellar density has dropped significantly and our originally assumed value of the density in the unburned material is no longer valid. Thus if no detonation is observed after an elapsed time  $\tau_h$  it is fair to conclude that, for the conditions investigated, no detonation can occur. We use a value of  $\tau_h = 0.02$  s which is consistent with estimates from direct numerical calculations of exploding Chandrasekhar-mass white dwarfs (Reinecke et al. 1999).

In Figure 3 we see how a spontaneous wave is initiated (at a density of  $2.3 \times 10^7$  g cm $^{-3}$ , a fuel composition of  $X(^{12}\text{C}) = X(^{16}\text{O}) = \frac{1}{2}$ , and a turbulent velocity of  $u'(L) = 0.2 \times 10^8$  cm s $^{-1}$ ) and propagates along the temperature gradient. However, after an elapsed time of  $0.02$  s =  $\tau_h$ , it does not pile up to a detonation. Instead it moves with a constant velocity at constant pressure.

On the other hand, Figure 4 shows the evolution from an initial isobaric state to a detonation. The initial conditions correspond to a turbulent velocity of  $u'(L) = 0.9 \times 10^8$  cm s $^{-1}$  at a density of  $2.3 \times 10^7$  g cm $^{-3}$  and a carbon mass fraction of  $\frac{1}{2}$ . The initial flame profile immediately develops a spontaneous burning front propagating along the spatial gradient of induction timescales. The wave gradually accel-

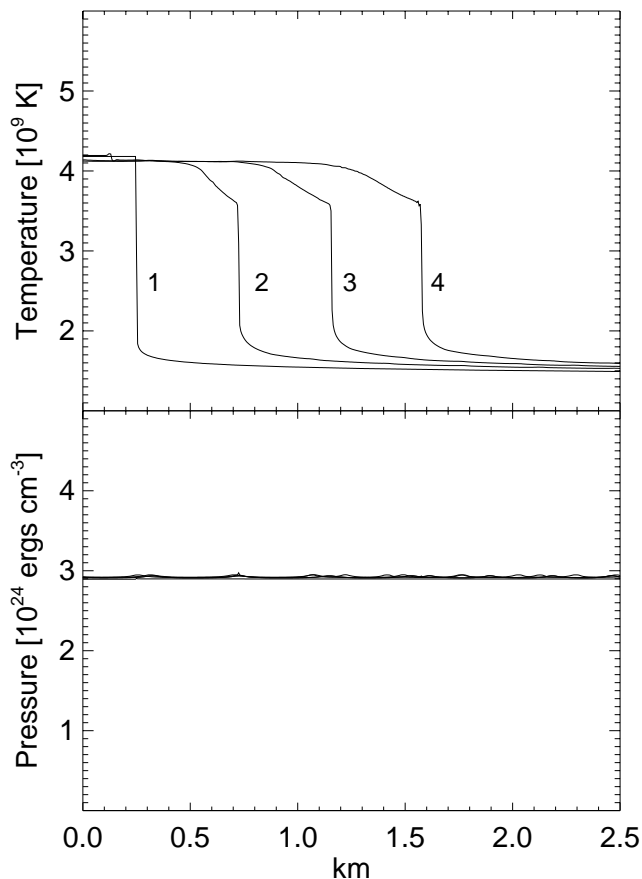


FIG. 3.—Evolution of a spontaneous flame which does not lead to a detonation. The matter has a density of  $2.3 \times 10^7$  g cm $^{-3}$  with a carbon mass fraction of  $\frac{1}{2}$ , and turbulent velocity is  $0.2 \times 10^8$  cm s $^{-1}$ . The numbers indicate subsequent times of the evolution: (1) 0 s, (2) 0.01 s, (3) 0.015 s and (4) 0.02 s.

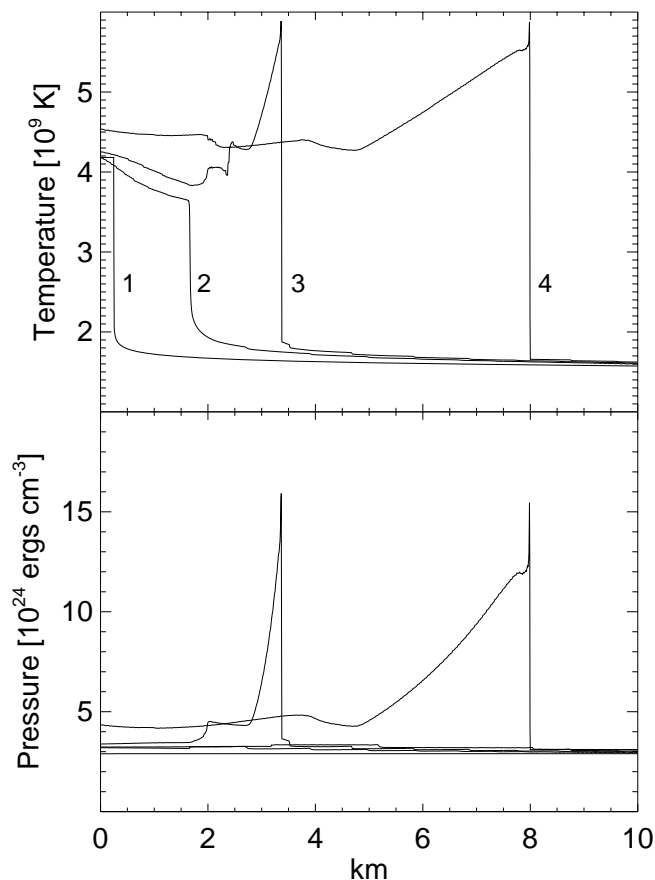


FIG. 4.—Evolution to a detonation at a density of  $2.3 \times 10^7$  g cm $^{-3}$ , a carbon mass fraction of  $\frac{1}{2}$ , and a turbulent velocity of  $0.9 \times 10^8$  cm s $^{-1}$ . The numbers indicate subsequent times of the evolution: (1) 0 s, (2) 0.002 s, (3) 0.0028 s, and (4) 0.0032 s.

erates, and at a certain velocity the burning mode switches to a detonation.

Our results are summarized in Table 1, where we give the turbulent velocity  $u'(L)$  necessary for the emergence of a detonation out of certain initial conditions. The latter are parametrized by the density and the nuclear composition of the unburned matter. The values given in Table 1 are all obtained from numerical simulations performed in planar geometry. In spherical geometry—due to spherical damping—these limits in terms of  $u'$  become higher.

We find that even under assumptions in favor for a DDT the velocities are always higher than those expected in Type

TABLE 1  
LIMITING THRESHOLD FOR TURBULENT VELOCITY  $u'(L)$  AT  
GIVEN  
DENSITY AND FUEL COMPOSITION

$u'(L)$ (cm s $^{-1}$ )	$\rho$ ( $\times 10^7$ g cm $^{-3}$ )	$X(^{12}\text{C})$	$X(^{16}\text{O})$
$> 0.5 \times 10^8$ .....	2.3	0.5	0.5
$> 0.6 \times 10^8$ .....	1.3	0.5	0.5
$> 0.8 \times 10^8$ .....	0.8	0.5	0.5
$> 0.25 \times 10^8$ .....	2.3	0.75	0.25
$> 0.3 \times 10^8$ .....	1.3	0.75	0.25
$> 0.4 \times 10^8$ .....	0.8	0.75	0.25
$> 0.9 \times 10^8$ .....	2.3	0.25	0.75
$> 10^8$ .....	1.3	0.25	0.75
$> 10^8$ .....	0.8	0.25	0.75

Ia supernovae. This observation suggests that a DDT could in principle only happen in the presence of stronger turbulent velocity fluctuations than the “typical” maximum value of  $10^7 \text{ cm s}^{-1}$ , which results for Rayleigh-Taylor-driven turbulence. This conclusion holds for equal fractions of C and O and also for mixtures enriched in carbon, although in the latter case the constraint is weakened.

#### 4. CONCLUSIONS

As a main result of our modeling we conclude that a transition from deflagration to detonation triggered by turbulent mixing seems to be a possibility only if significantly more kinetic energy is stored in turbulence. Our thresholds for the minimum values necessary for a DDT are all larger than the expected maximum rms turbulent velocities obtained from numerical simulations of the explosion. Since we started from the most optimistic assumptions

(ignoring strong fluctuations or geometrical effects such as spherical damping), we conclude that in more realistic models these limits would become even higher. On the other hand, going to higher turbulent velocity fluctuations would then cause even stronger fluctuations in temperature and fuel composition, leading to a situation where a transition to detonation would become practically impossible, as argued by Niemeyer (1999). Thus it turns out that a DDT based on the Zeldovich gradient mechanism must be regarded as a very unlikely scenario in Type Ia supernovae.

The authors thank M. Reinecke for providing us with the latest version of PROMETHEUS. This work was supported by the Deutsche Forschungsgemeinschaft and the Deutscher Akademischer Austauschdienst. A. M. L. also kindly acknowledges partial support by the NSF grants INT-9726315 and AST-3731569.

#### REFERENCES

- Fryxell, B. A., Müller, E., & Arnett, W. D. 1989, Max-Planck-Institut für Astrophysik Report 449, Garching  
 Höflich, P., Khokhlov, A. M., Wheeler, J. C., Phillips, M. M., Suntzeff, N. B., & Hamy, M. 1996, *ApJ*, 472, L81  
 Imshennik, V. S., Kal'yanova, N. L., Koldoba, A. V., & Chechetkin, V. M. 1999, *Astron. Lett.*, 25, 206  
 Khokhlov, A. M. 1991, *A&A*, 246, 383  
 Khokhlov, A. M., Oran, E. S., & Wheeler, J. C. 1997, *ApJ*, 478, 678  
 Niemeyer, J. C. 1999, *ApJ*, 523, L57  
 Niemeyer, J. C., & Woosley, S. E. 1997, *ApJ*, 475, 740  
 Reinecke, M., Hillebrandt, W., & Niemeyer, J. C. 1999, *A&A*, 347, 739  
 Timmes, F. X., & Woosley, S. E. 1992, *ApJ*, 396, 649  
 Zeldovich, Ya. B., Librovich, V. B., Makhviladze, G. M., & Sivashinsky, G. I. 1970, *Acta Astron.*, 15, 313